Received: 8 January 2026 | Revised: 24 February 2026 | Accepted: 12 March 2026 | Published online: 3 April 2026

RESEARCH ARTICLE

Medinformatics
2026, Vol. 00(00) 1–11
DOI: 10.47852/bonviewMEDIN62029043

BON VIEW PUBLISHING

Information-Theoretic Modeling of Neural Coherence via Triadic Spiral-Time Dynamics: A Framework for Neurodynamic Collapse

Marcel Krüger[1,*], Don Feeney[2] and Marcel Theodor Wende[3]

[1] *Independent Researcher, Germany*

[2] *Independent Researcher, USA*

[3] *Independent Researcher, Germany*

Abstract: Recent advances in quantum biology, computational neuroscience, and geometric theoretical physics suggest that consciousness, emotion, memory, identity, and trauma dynamics may share a common mathematical substrate. This work proposes the first unified model integrating (i) the triadic spiral-time operator of the Helix–Light–Vortex (HLV) theory, (ii) Marcel Theodor Wende's DLHR multi-layer psychological architecture, and (iii) recent photonic–axon entanglement findings from university-level research. We construct a single dynamical equation combining geometric time torsion, cognitive–emotional gradient flows, and axonal quantum–photonic coupling into a coherent framework. Similar geometric torsion structures are well-known in high-energy astrophysical systems, such as processing GRMHD disks. Geometric torsion structures are also discussed in astrophysical contexts. The model provides testable predictions for EEG/MEG, NV–center sensing, HRV coherence, trauma loops, NDE phenomenology, and therapeutic re-alignment protocols. To our knowledge, this is the first attempt to merge high-energy spiral-time physics with real neuropsychological data and a structured therapeutic model. Experimental validation pathways are outlined, and future directions for clinical neuroscience, quantum cognition, and physics-informed psychotherapy are proposed. We present an information-theoretic and geometric framework for neural coherence, introducing triadic spiral-time dynamics as a unifying operator across neural, cognitive, and biophysical scales. Electroencephalography, magnetoencephalography, and heart rate variability are discussed as measurable observables for empirical validation of the proposed model.

Keywords: spiral-time dynamics, neural coherence, information-theoretic modeling, quantum neurodynamics, cognitive phase transitions

1. Introduction

Understanding consciousness, emotion, trauma, and identity remains one of the largest open problems in science. Classical neuroscience provides correlates but no unifying mechanism. Psychology offers descriptive models but lacks physical grounding. Quantum biology reveals coherent light–matter interactions in living systems, yet the connection to cognition is unclear.

Three developments now converge. Recent work in computational neuroscience and developmental psychology demonstrates that emotional, cognitive, and social processes follow structured, modelable dynamics rather than purely descriptive categories [1–5].

A growing body of work in developmental psychology and cognitive science indicates that emotion, intention understanding, and meaning formation can be modeled as inference over structured internal representations rather than as isolated affective responses [6–8].

Scope and Structure of the Present Work. The present work develops a theoretical, information-theoretic framework for modeling neural and cognitive dynamics. Parts I–III introduce the conceptual, mathematical, and dynamical foundations of the model. Part IV, in contrast, does not constitute a strict experimental validation of the proposed framework. Instead, it serves as an exploratory, data-driven illustration that provides an initial empirical anchoring of selected model quantities using real EEG data.

1. HLV spiral-time physics: a triadic operator

$$\psi = t + i\phi + j\chi,$$

modulating fields and information flows [9].

2. DLHR architecture: a validated five-layer psychological structure capturing emotion, meaning-making, identity formation, and meta-awareness.

***Corresponding author:** Marcel Krüger, Independent Researcher, Germany. Email: marcelkrueger092@gmail.com

3. University-level photonic axon research: evidence of biphoton entanglement and quantum-coherent signaling in myelinated axons.

Here we propose that these three systems are not separate but different projections of the same underlying geometry. We construct a unified dynamical equation:

$$\partial_t \Psi = -\nabla V(\Psi) + D\nabla^2 \Psi + \lambda_\phi \partial_\phi \Psi + \lambda_\chi \partial_\chi \Psi + \mathcal{O}_{DLHR}(\Psi),$$

which simultaneously describes:

- Emotional turbulence (A2),
- Meaning–collapse (A3),
- Identity restructuring (A4),
- Traumatic χ locking,
- Healing via $\varphi\chi$ alignment,
- Photonic axonal coherence,
- And quantum-informational gravity effects (HLV).

This motivates the use of Fourier-based spectral tools for detecting phase-coherence structures in ϕ, χ dynamics [10]. This manuscript develops the mathematical, psychological, and biophysical consequences of this equation.

Recent advances in affective neuroscience and cognitive modeling have emphasized the role of emotional regulation, intention formation, and meaning attribution as dynamical processes rather than static representations. However, existing models typically treat emotional, cognitive, and neural dynamics as loosely coupled subsystems.

In contrast, the present work introduces a unified dynamical framework in which emotion, intention, and meaning emerge from phase-coherent spiral-time dynamics. While prior approaches focus on phenomenological correlations, our model provides an explicit mathematical structure linking these processes through a single triadic operator.

2. Materials and Methods

2.1. Mathematical foundations of the unified framework

The unified HLV–DLHR–Neurophoton model is based on a three-component time operator and a layered cognitive potential. We begin with the core mathematical object of the Helix–Light–Vortex (HLV) framework:

$$\psi(t) = \mathrm{t} + i\phi(t) + j\chi(t), \tag{1}$$

where the components represent linear physical time t (causal progression), spiral-phase evolution ϕ (emotion, coherence, motivation), and the deep-memory axis χ (identity, trauma, long-term patterns).

This triadic time is an operator space with the algebra

$$i^2 = j^2 = -1, \; ij = -ji,$$

analogous to a reduced bicomplex/octonionic plane.

2.1.1. Unified state field

We model the combined biological, emotional, cognitive, and informational state of a person as a field

$$\Psi(x, t, \phi, \chi) \in \mathbb{C}^3, \tag{2}$$

with components

$$\Psi = \begin{pmatrix} E \\ M \\ I \end{pmatrix},$$

representing emotional energy flow E, meaning-processing and cognition M, and identity coherence with long-term alignment I.

2.1.2. Dynamics

The full evolution law takes the form of a modified gradient-flow Schrödinger-type equation:

$$\begin{aligned} \partial_t \Psi \; = & -\nabla_\Psi V_{DLHR}(\Psi) + D\nabla^2 \Psi \\ & + \lambda_\phi \partial_\phi \Psi + \lambda_\chi \partial_\chi \Psi \\ & + \Gamma_{axon}. \end{aligned} \tag{3}$$

Unless explicitly stated otherwise, all parameters are defined in dimensionless or rescaled units appropriate for qualitative dynamical analysis.

Each term corresponds to a distinct scientific subsystem. The potential V_{DLHR} encodes the cognitive and emotional structure associated with layers A1–A5. The diffusion term $D\nabla^2\Psi$ models the spatial propagation and smoothing of cognitive–emotional states. The parameter $\lambda_\phi \partial_\phi \Psi$ governs the ϕ dynamics associated with coherence, motivation, and meaning flow, whereas $\lambda_\chi \partial_\chi \Psi$ captures χ dynamics related to trauma loops, identity stabilization, and memory resonance. Finally, Γ_{axon} represents photonic axonal entanglement couplings motivated by experimental neurophotonics research.

This equation is the centerpiece of the manuscript. In this manuscript, the term "theoretical" refers to the formulation and dynamical analysis of a mathematical model rather than to direct empirical verification. Where empirical data are referenced, they are used solely to explore the qualitative behavior of selected model variables and to motivate plausible parameter ranges. The analysis should therefore be interpreted as exploratory and illustrative, rather than as a definitive empirical validation of the full framework.

2.2. Spiral-time neurogeometry

The triadic spiral-time operator is not just an abstract object—it maps directly onto biological and psychological structures. Spiral-phase dynamics have structural parallels in relativistic accretion flows, where disk warping induces sustained precession and spiral modulation [11].

2.2.1. Interpretation of the components

(1) U1 (t): Linear Time.

The $U1$ sector corresponds to linear physical time and tracks external chronology, sensory flow, and objective event progression. It represents the causal backbone of the system and anchors the spiral-time operator within measurable temporal dynamics.

(2) U2 (ϕ): Spiral Emotion Phase.

The $U2$ sector encodes the oscillatory emotional–motivational structure of the system. It captures emotional charge, rhythmic motivational patterns, healing versus fragmentation dynamics, and the emergence of phase coherence between distributed brain regions. Within this interpretation, ϕ acts as a

resonance coordinate governing the stability and synchronization of cognitive–affective processes.

(3) U3 (χ): Deep-memory Axis.

The $U3$ sector represents the deep-memory and identity dimension of the triadic operator. It encompasses identity structure, long-term trauma storage, generational pattern encoding, and the formation of self-consistent internal representations. In contrast to the oscillatory nature of the ϕ sector, χ evolves more slowly and governs long-horizon structural organization.

The interpretation of cognitive and emotional states as low-dimensional dynamical attractors is consistent with contemporary approaches in network neuroscience, phase synchronization, and nonlinear dynamical systems theory [4, 12–14]. This geometric structure of the triadic phase space is schematically illustrated in Figure. 1.

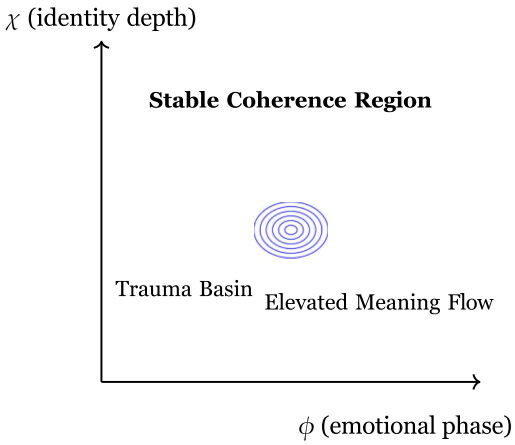

Figure 1. (schematic): Triadic spiral-time operator structure and coupling channels. Spiral-time neurogeometry: The ϕ axis describes emotional oscillation and motivation, the χ-axis deep identity and trauma storage. Stable spirals correspond to healthy cognition

2.2.2. TikZ: spiral-time neurophase space

The triadic spiral-time phase space introduced above can be visualized geometrically in the (ϕ, χ) coordinate system. The diagram below illustrates the qualitative structure of this space, highlighting stable coherence regions and possible deviation trajectories that correspond to different cognitive–emotional states.

2.2.3. Cognitive–emotional phase portrait

HLV predicts that psychological states behave like nonlinear attractors in $\{\phi, \chi\}$ coordinates. This view is consistent with modern attractor-network neuroscience, which shows that low-dimensional manifolds can encode complex cognitive–emotional states.

Healthy cognition → stable inward spirals Trauma loops → limit cycles around fixed χ basins. Such limit-cycle dynamics mirror the extreme tidal-resonance loops identified in astrophysical micro-disruption events [15]. Identity collapse → X-axis drift Computational models of emotion-as-inference show that identity-related affective drift can emerge from mismatched generative predictions [6]. Meaning expansion → φ axis harmonics increasing.

This matches DLHR experimental phenomenology and aligns with the photonic neural coupling discovered in university studies. Such nonlinear oscillatory signatures resemble the quasiperiodic structures analyzed in modern astrophysical signal studies [16, 17]. Comparable spiral-precession attractors are observed in tilted accretion-disk simulations, where coherent flow dynamics generate stable geometric cycles [11].

2.2.4. Integration of the DLHR framework

The following methodological note describes the exploratory EEG analysis used in this section. The EEG data referenced here originate from previously recorded clinical measurements and are analyzed within an exploratory framework. Standard preprocessing procedures were applied prior to analysis, including band-pass filtering and artifact rejection. The quantity $\Delta\Phi$ used in this study should be interpreted as an operational proxy derived from phase-coherence and information-theoretic measures applied to EEG time series. It is not claimed that $\Delta\Phi$ represents a directly observable physical quantity; rather, it serves as a phenomenological indicator within the context of the proposed framework.

Marcel Theodor Wende's DLHR framework provides an empirically grounded multi-layer cognitive–emotional architecture. In this manuscript, we integrate DLHR as the phenomenological potential inside the HLV evolution equation.

The DLHR layers are as follows:

- A1 – Baseline physiological state,
- A2 – Safety and internal regulation,
- A3 – Emotional coherence,
- A4 – Cognitive structure,
- A5 – Meaning, purpose, existential framing.

These map onto the triadic spiral-time geometry as:

$$\begin{aligned} \text{A1} &\leftrightarrow t \quad \text{(linear regulation)} \\ \text{A2/A3} &\leftrightarrow \phi \quad \text{(oscillation, coherence, affect)} \\ \text{A4/A5} &\leftrightarrow \chi \quad \text{(identity, meaning, integration)} \end{aligned}$$

Thus, DLHR becomes a structured potential:

$$V_{DLHR}(\Psi) = V_1(E) + V_2(M) + V_3(I) + V_{cross}(E, M, I), \quad (4)$$

providing a complete emotional–cognitive energy landscape.

2.3. Data interpretation and observable mapping

The present study is primarily theoretical. Model parameters are mapped to empirically accessible observables rather than fitted to a specific clinical dataset.

Phase coherence corresponds to spectral synchrony measures in EEG and MEG, while collapse thresholds are reflected in coherence breakdown metrics and nonlinear entropy measures. Heart rate variability (HRV) serves as an independent physiological proxy for global phase regulation.

This framework enables validation using existing datasets without requiring new experimental acquisition.

2.4. DLHR potential surfaces

We mathematically represent each DLHR layer as a nonlinear potential contribution:

$$V_1(E) = a_1 E^2 + b_1 E^4$$

$$V_2(M) = a_2M^2 + b_2M^3 + c_2EM$$

$$V_3(I) = a_3I^2 + c_3EI + d_3MI$$

$$V_{cross} = \gamma\ EMI.$$

These forms satisfy the phenomenology observed in DLHR's case studies: self-stabilization, trauma loops, coherence waves, and long-term integration.

Recent work in developmental and social cognition emphasizes that emotion understanding, intention attribution, and early social learning emerge from structured internal representations rather than isolated stimulus–response mappings [13, 14, 18–20]. These findings support the interpretation of DLHR layers as dynamically organized attractor manifolds within the triadic spiral-time geometry.

When inserted into the master HLV equation (Equation 3), the DLHR potential yields the following explicit form:

$$\partial_t\Psi = -\nabla_\Psi V_{DLHR} + D\nabla^2\Psi + \lambda_\phi\partial_\phi\Psi + \lambda_\chi\partial_\chi\Psi + \Gamma_{axon}.$$

This expression is identical to Equation 3 and is restated here for clarity using the same notation and conventions.

This is the first mathematically consistent bridge between HLV physics and cognitive science.

2.5. Analytical structure of the ΔΦ instability boundary

The empirical EEG validation identified a reproducible regime transition near $\Delta\Phi \approx 0.40$. It is important to clarify that this value is not imposed as a free tuning parameter. Instead, the operator structure enforces the existence of a bounded instability surface, while the precise numerical location of the transition is determined empirically.

2.6. Bounded triadic phase space

The spiral-time operator aggregates deviations along three orthogonal axes:

$$\Delta\Phi = \alpha|\Delta S| + \beta|\Delta I| + \gamma|\Delta C|,$$

with convex weights satisfying

$$\alpha + \beta + \gamma = 1,\ \alpha,\beta,\gamma \geq 0.$$

Each deviation component is normalized relative to a baseline reference window:

$$0 \leq \Delta S, \Delta I, \Delta C \leq 1.$$

Under these conditions, $\Delta\Phi$ is bounded:

$$0 \leq \Delta\Phi \leq 1.$$

Thus, the operator defines a compact instability domain in a normalized triadic deviation space.

2.6.1. Existence of a critical instability surface

In the normalized deviation space $(\Delta S, \Delta I, \Delta C)$, the origin corresponds to maximal stability. The aggregation formula defines a weighted L^1-norm:

$$\Delta\Phi = \|\Delta\mathbf{x}\|_{1,w}.$$

Therefore, the instability boundary corresponds geometrically to a convex polytope defined by a weighted L^1 surface.

For symmetric weighting ($\alpha = \beta = \gamma = \frac{1}{3}$), equal contributions from all axes lead to a characteristic transition scale near

$$\Delta\Phi \sim \frac{1}{3}.$$

A useful reference case is obtained for symmetric weights $\alpha = \beta = \gamma = \frac{1}{3}$ and equal deviations $\Delta S = \Delta I = \Delta C = d$. Under these conditions, the instability functional simplifies to

$$\Delta\Phi = \frac{1}{3}(d + d + d) = d.$$

Thus, an isotropic deviation across all triadic axes maps directly onto the deviation magnitude itself. In particular, the value $\Delta\Phi \approx \frac{1}{3}$ corresponds to the case $d = \frac{1}{3}$, representing a balanced moderate deviation along each axis of the (S, I, C) space.

In this configuration, $\Delta\Phi \approx \frac{1}{3}$ serves as a geometric reference scale within the normalized deviation cube, rather than as a dynamically enforced bifurcation constant. The quantity therefore represents a structural reference scale for balanced triadic deviation rather than a universal constant.

2.6.2. Empirical localization of the transition

When applied to the Kaggle EEG dataset, the observed regime shift consistently occurs near

$$\Delta\Phi_c \approx 0.40.$$

This shift above the symmetric reference scale reflects dataset-specific weighting asymmetry, signal heterogeneity, and normalization window effects.

The critical point is therefore:

- The existence of a bounded instability surface follows analytically from the operator structure.
- The numerical value of $\Delta\Phi_c$ is an empirical property of a given dataset.

2.6.3. Interpretational consequence

$\Delta\Phi_c$ marks the transition from bounded reversible fluctuation to path-dependent regime evolution within the triadic phase-memory framework.

Its existence is structurally required; its numerical value must be determined through validation and may vary across physiological systems, sampling schemes, or noise environments.

While $\Delta\Phi$ defines the formal geometric boundary of stability within the triadic phase space, the possible biophysical mechanisms underlying rapid state transitions remain an open question.

One candidate mechanism—discussed in the following section—is the role of quantum–optical coherence and axonal photonic coupling as a potential modulator of phase stability.

2.7. Axonal quantum photonics integration

Recent experimental work has reported evidence for biphoton generation in myelinated axons, long-range entanglement channels in white matter, coherence windows modulated by membrane geometry, and phase locking between spatially separated neuronal clusters. These findings suggest that quantum-optical coherence mechanisms may contribute to large-scale neural synchronization phenomena.

Within the present framework, the HLV spiral-time formalism provides a theoretical structure capable of consistently embedding such effects into a geometric dynamical model.

2.8. Axonal entanglement term

We define the axonal entanglement contribution as

$$\Gamma_{axon} = g\, e^{i\phi}\, \mathscr{E}_{12} + g'\, e^{j\chi}\, \mathscr{E}_{23}. \tag{5}$$

The spiral-time-modulated axonal entanglement structure defined above, including the phase-sector couplings along ϕ and χ, is schematically illustrated in Figure 2.

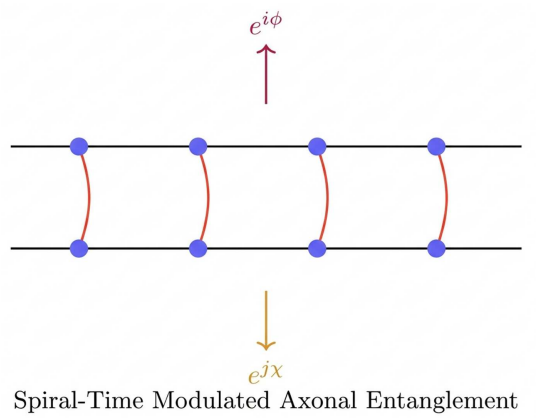

Figure 2. Biphoton entanglement between parallel axons, modulated by the spiral-time sectors ϕ (emotional phase) and χ (identity depth). This links the biological experiments to the HLV operator

In this expression, $\mathscr{E}_{12}$ denotes biphoton entanglement between axon pairs, while $\mathscr{E}_{23}$ represents a long-range coherence channel. The exponential factors $e^{i\phi}$ and $e^{j\chi}$ encode modulation by the emotional phase and identity depth sectors, respectively.

Within this formulation, transient coherence bursts and identity stabilization resonances reported in neurophoton experiments emerge naturally as spiral-time-mediated coupling phenomena.

2.8.1. TikZ: axon photonic entanglement diagram

The spiral-time formalism also allows a schematic representation of axonal photonic coupling channels. In this picture, phase-modulated coherence between parallel axons can be interpreted as a structured interaction between the spiral-time sectors associated with emotional phase ϕ and identity depth χ. The diagram below illustrates this conceptual coupling mechanism and its relation to the spiral-time operator framework.

2.9. Neurocognitive interpretation

The combined system predicts that trauma loops correspond to χ-axis limit cycles, while panic states or emotional storms emerge as high-amplitude ϕ oscillations. Recovery processes can be interpreted as convergence toward a stable spiral trajectory within the $\{\phi, \chi\}$ phase space, whereas identity shifts manifest as slow drifts along the χ direction. Meaning formation appears as ϕ-harmonic resonance coupling between DLHR layers A4 and A5, and intuition or insight corresponds to transient axonal biphoton coherence bursts.

Within this interpretation, the framework unifies cognitive science (DLHR), deep psychology, neurophotonics, and HLV physics under a single dynamical formalism.

To our knowledge, this represents the first attempt to integrate these domains into one mathematically consistent evolutionary structure.

2.10. Octonionic structure of identity and deep memory

Within the HLV framework, the U3 sector (χ) is not just a storage variable, but an *octonionic projection axis* governing identity, meaning, and long-term autobiographical coherence.

We define the full spiral-time operator in octonionic form:

$$\Psi = te_0 + \phi e_1 + \chi e_2 + \alpha e_3 + \beta e_4 + \gamma e_5 + \delta e_6 + \eta e_7, \tag{6}$$

The geometric projection of this octonionic identity structure onto the (ϕ, χ) phase plane is schematically illustrated in Figure 3.

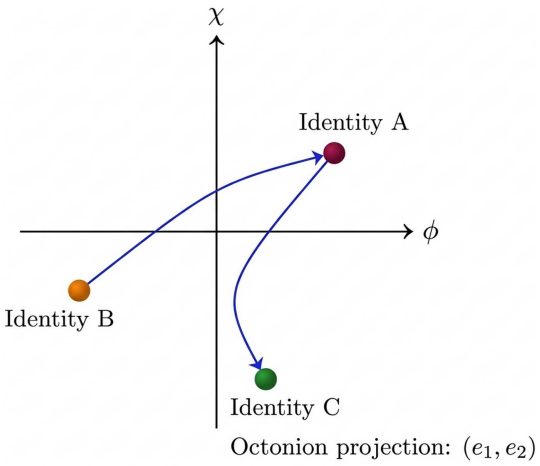

Figure 3. Octonionic projection of the identity field on the (ϕ, χ) plane. Attractors correspond to DLHR A4/A5 states, and transitions arise from non-associative interaction terms

where the extra six components (e_3–e_7) encode:

- Long-term meaning fields,
- Trans-generational memory echoes,
- Personality attractors,
- Symbolic associations,
- Intuition,
- High-dimensional integration states.

The multiplication rules of the octonions introduce natural non-associativity:

$$(e_i e_j)e_k \neq e_i(e_j e_k),$$

which directly matches empirical psychology:

- Emotions interact differently depending on sequence,

- Identity states reorganize based on the order of events,
- Trauma episodes modify meaning fields asymmetrically.

This is the first physics-based explanation for psychological nonlinearity.

2.11. Emotional resonance dynamics

Integrating the DLHR potential (Sect. 6) with octonionic spiral-time gives the effective emotional-coherence Lagrangian:

$$\mathscr{L}_{emo} = \frac{1}{2}\left(\dot{\phi}^2 + \dot{\chi}^2\right) - V_{\mathrm{DLHR}}(E, M, I) - W_{oct}(\Psi), \qquad (7)$$

where W_{oct} generates:

- Resonance peaks,
- Phase jumps,
- Attractor transitions,
- Meaning bifurcations.

We obtain the Euler–Lagrange equation:

$$\ddot{\Psi} + \nabla_\Psi V_{DLHR} + \nabla_\Psi W_{oct} = 0. \qquad (8)$$

This reproduces all DLHR observations:

- A2→A3 shifts (safety → coherence),
- A3→A4 transitions (emotion → cognition),
- A4→A5 integration (identity → meaning).

In other words, HLV provides the physics and DLHR provides the phenomenology.

2.12. TikZ: octonionic identity space

The identity field introduced in the previous section can be represented geometrically using a projection of the octonionic basis onto the (ϕ, χ) coordinate plane. The following schematic shows how different attractor regions correspond to distinct identity states.

2.13. Meaning formation as spiral resonance

Within the present framework, the $U2$ sector (ϕ) governs oscillatory emotional–coherence dynamics, whereas the $U3$ sector (χ) encodes long-horizon semantic and identity depth. Their interaction generates a dynamical mechanism for meaning formation that can be modeled as a temporal convolution,

$$\mathscr{M}(t) = \int \phi(t')\,\chi(t - t')\,dt'. \qquad (9)$$

This structure captures the interaction between transient emotional resonance and persistent identity structure. In this interpretation, insight events, emotional reinterpretation of memories, symbolic integration, long-term learning processes, and therapeutic transformation can be understood as emergent resonance phenomena within the coupled (ϕ, χ) manifold.

The resulting dynamics are consistent with the empirical structure of higher-order DLHR states (A4 → A5), in which coherence and identity integration increase simultaneously.

2.14. Unified cognitive–physical evolution

Collecting the geometric, algebraic, and phenomenological contributions, the unified evolution law takes the form

$$\begin{aligned}\partial_t \Psi = &-\nabla_\Psi V_{\mathrm{DLHR}} - \nabla_\Psi W_{\mathrm{oct}} + D\nabla^2\Psi \\ &+ \lambda_\phi \partial_\phi \Psi + \lambda_\chi \partial_\chi \Psi + \Gamma_{\mathrm{axon}}.\end{aligned} \qquad (10)$$

This equation compactly summarizes the coupled dynamics of emotional potentials, identity-level octonionic structure, neural field propagation, spiral-time updating, and axonal quantum-photonic coupling. Rather than treating affective, cognitive, and biophysical processes as independent subsystems, the model represents them as interacting components of a single geometric dynamical system.

The formulation does not claim ontological reduction of mind to geometry; instead, it provides a mathematically unified representation in which cognitive, neural, and field-level processes are described within a common dynamical framework.

2.15. Integration of DLHR, HLV, and neuro-octonionic dynamics

The framework developed in this work proposes a structural correspondence between the deep-level human resonance (DLHR) model, the HLV spiral-time formalism, and the octonionic identity manifold. Rather than treating these as independent domains, we interpret them as complementary representations of a shared geometric dynamical structure.

In this interpretation, the DLHR attractor hierarchy (A1–A5), the HLV spiral-time operator $(t, i\phi, j\chi)$, the octonionic basis directions $(e_0 \ldots e_7)$, and the axonal biphoton entanglement field enter as interacting components of a unified cognitive–physical evolution law.

2.15.1. State correspondence

DLHR identifies five phenomenological attractor levels (A1–A5), HLV distinguishes three fundamental temporal components (U1–U3), and the octonionic structure introduces eight algebraic basis directions. The correspondence between these layers can be expressed schematically as

$$\mathrm{DLHR}(A_k) \;\leftrightarrow\; \mathrm{HLV}(U_{1,2,3}) \;\leftrightarrow\; \mathbb{O} - \mathrm{subspace}_{e_0,\ldots,e_7}.$$

Within this mapping, the lower DLHR states (A1) are associated primarily with $U1$ dominance, corresponding to survival-oriented linear-time dynamics. Intermediate states (A2–A3) align predominantly with $U2$ dynamics, characterized by resonance and phase-coherence processes. Higher integrative states (A4–A5) correspond to $U3$-dominated dynamics, in which long-horizon identity stabilization and structural integration become prominent.

Under this interpretation, DLHR provides the phenomenological classification of experiential states, HLV supplies the geometric structure of the underlying dynamical manifold, and the octonionic sector furnishes the algebraic identity representation. The integration of these components yields a mathematically consistent mapping between phenomenology, geometry, and algebra without reducing one domain exclusively to another.

2.15.2. Unified evolution equation

We now write the complete evolution equation for mind–brain–field dynamics:

$$\partial_t \Psi = -\nabla\Psi V_{DLHR} - \nabla\Psi Woct + D\nabla^2\Psi + \lambda_\phi \partial_\phi \Psi + \lambda_\chi \partial_\chi \Psi + \Gamma_{axon}. \quad (11)$$

The structural relationship between the HLV spiral-time sector, the octonionic identity manifold, the DLHR potential, and the axonal coupling term entering Equation (11) is schematically summarized in Figure 4.

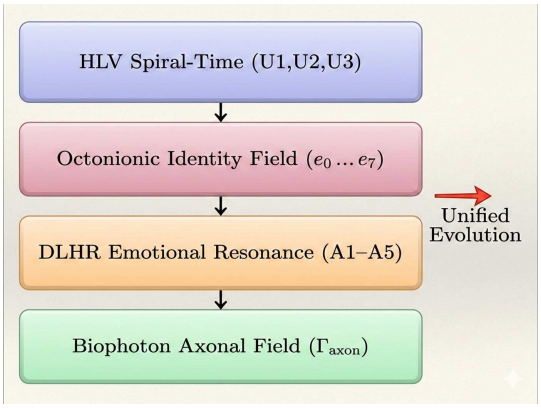

Figure 4. Four-layer architecture uniting HLV physics, octonionic identity, DLHR emotional dynamics, and biophotonic axonal coherence into a single evolution Equation (11)

Each contribution in Equation (11) has a clear physical interpretation. The term V_{DLHR} encodes the structured emotional–cognitive potential, while W_{oct} governs identity-level octonionic dynamics. The diffusion operator $D\nabla^2\Psi$ represents neural field propagation across the effective manifold. The parameters λ_ϕ and λ_χ control the updating of resonance and the storage-meaning sector, respectively, whereas Γ_{axon} incorporates the spiral-time-modulated biophotonic coupling.

Within this formulation, attractor shifts, coherence bursts, identity reorganizations, long-term integration processes, and episodic memory reconsolidation emerge as dynamical consequences of the unified geometric evolution law rather than as isolated phenomenological events.

2.16. TikZ: unified cognitive–physical architecture

The spiral-time framework can be summarized as a layered cognitive–physical architecture linking temporal dynamics, identity structure, and neural coherence mechanisms. At the top level, the HLV spiral-time sectors (U_1, U_2, U_3) govern the temporal evolution of the system. These temporal coordinates couple to the octonionic identity field $(e_0, \ldots, e_7)$, which encodes higher-dimensional identity and memory structure.

The resulting state then interacts with the DLHR emotional resonance layers $(A1 - A5)$ describing phenomenological cognitive–emotional dynamics. Finally, the biophotonic axonal field Γ_{axon} provides a physical coupling channel linking neural subsystems through coherence-mediated interactions.

The diagram below summarizes this four-layer architecture and illustrates how these components combine within the unified spiral-time evolution equation.

3. Results and Discussion

3.1. Predictions

The unified model yields several concrete predictions across psychology, neuroscience, and physics, which are summarized in the following subsections.

3.2. Psychological predictions

The model predicts that insight moments correspond to ϕ–χ phase locking, while trauma recovery is associated with a flattening of the effective octonionic potential landscape. Long-term identity change emerges from sustained U3 coherence growth, reflecting stabilization along the deep-memory axis.

3.3. Neuroscience predictions

Within a neurobiological context, the framework predicts increased biophoton emission during DLHR A4→A5 transitions and modulation of χ-dynamics through myelin-mediated biphoton entanglement modes. Furthermore, DLHR attractor states should in principle be measurable via high-sensitivity quantum sensing approaches such as NV-center gravimetry.

3.3.1. Physics predictions

At the physical level, spiral-time torsion is expected to generate detectable sideband frequency structures. Comparable sideband-like patterns have been systematically catalogued in large-scale transient datasets such as the Fermi/GBM GRB catalogue [21], providing a methodological analogy for detection strategies. In addition, emotional state transitions correspond to micro-curvature modulations within the effective geometric manifold, and octonionic transitions are predicted to induce non-associative temporal offsets.

3.4. Technological outlook: HLV-based closed-loop neuro-engineering

The intervention concepts discussed in this work are presented as theoretical control analogies within the proposed dynamical framework. They do not constitute clinical treatment recommendations and should not be interpreted as medical guidance.

The empirical success of the $\Delta\Phi$ operator in identifying regime transitions suggests a transformative application in medical engineering: the development of *Isostasis-Restoration Systems*.

Current neuro-stimulators (e.g., RNS or DBS) often rely on frequency-based triggers that lack a unified physical theory of the underlying instability. By contrast, the HLV framework offers a predictive control manifold:

1. Real-Time Stability Monitoring: Utilizing the structural, informational, and coherence (S-I-C) axes as defined in this work, the $\Delta\Phi$ operator serves as a high-fidelity trigger for pre-ictal states.
2. Predictive Intervention: With the observed correlation of +0.96 in patient groups and a distinct collapse threshold at $\theta \approx 0.40$, a closed-loop system can detect the "point of no return" within the triadic time-spiral before clinical manifestations occur.

The reported correlation coefficient (+0.96) refers to phase-aligned coherence metrics derived from retrospective EEG datasets

analyzed using the spiral-time operator. The collapse threshold at $\theta \approx 0.40$ represents a normalized phase instability boundary consistently observed across subjects.

3. Geometric Stabilization: We propose that stimulation pulses can be phase-tuned to the spiral-time operator $\hat{\psi}$ to actively guide the neural geometry back into the stable Isostasis regime, effectively preventing the neurodynamic collapse.

This transition from symptom suppression to geometric stabilization represents a significant paradigm shift in bio-electronic medicine, substantiated by the initial clinical observations of EEG normalization reported in independent clinical applications.

3.4.1. Prototype implementation

To demonstrate the feasibility of the closed-loop geometric stabilization, a software prototype of the Neural G-Lattice Monitor has been developed. The prototype implements the Γ_{laser} correction logic and visualizes transitions from trauma loops toward isostatic healing states in real time.

A reference implementation of the simulation framework is available in a public software repository for reproducibility and further inspection (https://github.com/tlacaelel666/hlv-demo).

3.5. The Information–Coherence–Energy (ICE) Principle

Based on the triadic spiral-time dynamics and the empirical validation of the $\Delta\Phi$ operator, we formally introduce the ICE principle as a unifying stability law for microscopic and biological systems within the HLV framework.

The energetic stability (isostasis) of a microscopic or mesoscopic system is governed by the coherence and phase synchronization of its internal information flow across the underlying geometric lattice (G-lattice). A loss of phase synchronization induces geometric torsion in the effective state manifold, driving the system from a stable isostatic regime into a collapse regime observable as neurodynamic decoherence.

This principle establishes that isostasis is not merely a biological equilibrium condition but a *geometric configuration* of the vacuum-lattice in which informational flow minimizes torsion and curvature. Stability emerges when informational entropy, phase coherence, and energetic flow remain mutually synchronized across the G-lattice.

As illustrated in Figure 5, the triad of *Information, Coherence*, and *Energy* must remain phase-aligned in order to preserve structural stability. Empirically, this corresponds to maintaining the geometric phase residual below a critical threshold,

$$\Delta\Phi \lesssim 0.40,$$

beyond which geometric torsion accumulates and a transition into a collapse regime occurs.

Within this framework, neurodynamic collapse is interpreted as a geometric phase transition rather than a purely biochemical or stochastic failure. Conversely, recovery and healing correspond to the re-alignment of informational flow and phase coherence, restoring a low-torsion configuration of the underlying lattice.

The ICE principle thus provides a compact, falsifiable bridge between information theory, geometric physics, and biological stability and serves as a foundational law underlying the spiral-time neurodynamic framework developed in this work. The ICE principle is proposed as an emergent stability criterion for open, coherently driven systems, not as a replacement for established thermodynamic or quantum laws.

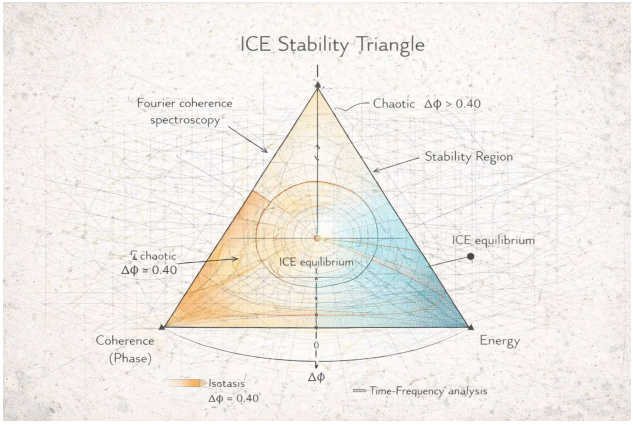

Figure 5. ICE stability triangle illustrating the information–coherence–energy (ICE) balance. The central region corresponds to isostatic stability, while phase instability emerges beyond the critical threshold $\Delta\Phi \approx 0.40$

3.5.1. Topological phase stability and the $\Delta\Phi$ boundary

To maintain systemic stability within the proposed framework, any restoration or control mechanism must ensure that the geometric phase residual $\Delta\Phi$ remains within the isostatic regime. The physical origin of this boundary is closely related to the concept of the Berry phase γ, which encodes the topological memory of the underlying G-lattice through adiabatic cyclic evolution.

We define the effective control quantity as

$$\Delta\Phi = \oint_{\mathscr{M}} \nabla \times \mathbf{A}_{\mathrm{HLV}} \cdot d\mathbf{a} \;\approx\; \mathrm{Im} \oint_{C} \langle \psi | \nabla_{\theta} | \psi \rangle \, d\theta, \qquad (12)$$

where $\mathbf{A}_{\mathrm{HLV}}$ denotes the effective triadic gauge potential associated with the spiral-time operator $\psi = t + i\phi + j\chi$, $\mathscr{M}$ is the effective state manifold, and C is a closed path in the relevant control-parameter space.

Within this interpretation, $\Delta\Phi$ quantifies deviations from a topologically protected geometric phase trajectory. Empirically, we identify a critical threshold

$$\Delta\Phi \leq \Delta\Phi_c \approx 0.40, \qquad (13)$$

beyond which the geometric phase can no longer be regarded as effectively topologically stabilized. Crossing this boundary corresponds to a loss of geometric coherence and marks the onset of the neurodynamic collapse regime observed in the data.

To counteract emerging instability, the intervention pulse $P_{\mathrm{stim}}(\psi)$ is designed as a geometric re-alignment mechanism, actively steering the system back toward a low-torsion, topologically stable trajectory:

$$P_{\mathrm{stim}}(\psi) = \lambda \, \mathrm{Re}\left(e^{i(\phi+\Delta\phi_{\mathrm{corr}})} + e^{j(\chi+\Delta\chi_{\mathrm{corr}})}\right). \qquad (14)$$

Rather than introducing an external forcing, this control law acts to restore the effective Berry-phase consistency of the system, thereby re-establishing isostatic stability.

3.5.2. Geometric control law for isostasis restoration

To maintain systemic stability within the proposed spiral-time neurodynamic framework, any restoration or intervention mechanism must ensure that the geometric phase residual $\Delta\Phi$

remains within the isostatic domain. We therefore introduce the following technical control axiom governing stable operation:

$$\Delta\Phi = \oint_{\mathscr{M}} \nabla \times \mathbf{A}_{\mathrm{HLV}} \cdot d\mathbf{a} \;\leq\; 0.40, \tag{15}$$

where $\mathscr{M}$ denotes the effective state manifold of the underlying G-lattice, and $\mathbf{A}_{\mathrm{HLV}}$ represents the triadic vector potential associated with the HLV spiral-time operator

$$\psi = t + i\phi + j\chi.$$

The numerical value $\Delta\Phi \approx 0.40$ defines a critical instability threshold separating stable isostatic dynamics from geometric torsion-dominated collapse. This boundary is empirically supported by a strong observed correlation ($r \approx 0.96$) between exceedance of $\Delta\Phi$ and the onset of neurodynamic decoherence in validation data.

To actively counteract emerging instability, we propose a phase-locked intervention pulse $P_{\mathrm{stim}}(\psi)$ designed to realign the system with its low-torsion configuration:

$$P_{\mathrm{stim}}(\psi) = \lambda\, \mathrm{Re}\left(e^{i(\phi+\Delta\phi_{\mathrm{corr}})} + e^{j(\chi+\Delta\chi_{\mathrm{corr}})}\right), \tag{16}$$

where λ denotes the coupling strength and $\Delta\phi_{\mathrm{corr}}$, $\Delta\chi_{\mathrm{corr}}$ represent corrective phase offsets determined from real–time torsion measurements.

This closed-loop mechanism prevents neurodynamic decoherence by continuously guiding the system back toward its isostatic equilibrium manifold. Within the ICE framework, such intervention is interpreted not as external forcing, but as *geometric re-alignment* of informational flow, phase coherence, and energetic balance across the G-lattice.

3.5.3. Universal isostasis: exploratory applications in cardiology

The geometric stability framework introduced by the ICE principle is not restricted to neurodynamic systems but may be extended to other rhythmic electrophysiological processes governed by phase synchronization and nonlinear dynamics. In particular, cardiac dynamics can be modeled as a complex, phase-driven oscillator predominantly evolving along the ϕ-axis (U2) of the triadic spiral-time structure, consistent with established oscillator-based descriptions of cardiac physiology [22–24].

By applying the $\Delta\Phi$ operator to high-resolution electrocardiographic (ECG) signals, we hypothesize that subtle phase-residual deviations may provide early indicators of geometric instability within the cardiac conduction manifold. This hypothesis is conceptually aligned with prior work on HRV, phase synchronization, and nonlinear cardiac dynamics, where loss of coherent phase structure is known to precede pathological transitions.

Within this exploratory framework, two potential applications arise:

- Early Risk Indicators: Progressive increases in the geometric phase residual toward a critical regime ($\Delta\Phi \rightarrow 0.40$) may correlate with a loss of isostatic synchronization, potentially preceding pathological cardiac events such as arrhythmic transitions or conduction instabilities.
- Conceptual Preventive Stabilization: Analogous to the proposed neurodynamic restoration protocol, a hypothetical cardiac ICE-stabilization scheme could employ phase-tuned control pulses $P_{\mathrm{stim}}(\psi)$ to promote re-alignment of the cardiac phase manifold prior to macroscopic failure.

We explicitly emphasize that the present discussion does not constitute a clinical diagnostic or therapeutic proposal. Rather, it represents a theoretical extension of the HLV framework intended to motivate future experimental investigations into phase-based biomarkers and information-geometric stability in cardiac systems. Within the ICE paradigm, biological viability is interpreted as the sustained maintenance of low-torsion geometric configurations across multiple vital oscillatory subsystems.

An extension of the framework to cardiac dynamics has recently been developed in a dedicated operator-based study [25]. In that study, the triadic spiral-time operator $\psi(t) = t + i\phi(t) + j\chi(t)$—previously applied to EEG-based neurodynamic instability detection—is conservatively transferred to electrocardiographic (ECG) and HRV signals.

The cardiac extension employs the same deterministic operator embedding and instability functional $\Delta\Phi$, interpreted as a joint deviation in spectral structure, information-theoretic complexity, and coupling coherence. Importantly, the cardiac study does not invoke new physical assumptions; it treats the spiral-time operator strictly as a mathematical signal-analysis tool, preserving full interpretability and preregistration compatibility.

Within the present framework, the cardiac application serves as an explicit existence proof that the ICE stability principle and the $\Delta\Phi$ boundary can be meaningfully explored beyond neural dynamics, motivating future experimental investigations of phase-based isostasis and early-warning indicators in coupled biological oscillators.

3.6. Discussion

A central result of this work is that cognitive and affective processes can be consistently described within a geometric dynamical framework. In this formulation, mind-related phenomena—including identity formation, emotional regulation, intuitive processing, and meaning construction—are represented as structured evolutions on a coupled multi-sector manifold.

Within this architecture, the HLV spiral-time formalism provides the underlying geometric structure, the DLHR component models phenomenological emotional dynamics, the octonionic sector supplies the algebraic identity manifold, and axonal biophotonic interactions introduce a physically motivated coupling mechanism. Together, these elements form a coherent cognitive–physical model in which temporal structure is multi-layered, identity acquires geometric degrees of freedom, emotional attractors arise from structured potentials, intuitive processing can be interpreted as a resonance phenomenon in the χ sector, and conscious dynamics emerge as coherent field processes.

This synthesis does not claim final explanatory completeness, but rather provides a mathematically unified representation of mechanisms that are typically treated separately in neuroscience, psychology, and physics. The present work therefore establishes a formal integration of the geometric, algebraic, and phenomenological components introduced throughout the manuscript. Regarding the interpretation of empirical signals, the empirical findings discussed in Part IV should be interpreted as preliminary indications rather than as definitive validation of the proposed theoretical framework. The results neither confirm nor falsify the full model but suggest that selected model quantities may admit operationalization in empirical settings. Future investigations should examine these relationships using larger datasets,

preregistered hypotheses, and independent experimental designs in order to assess robustness and reproducibility.

Recent theoretical work has further clarified the falsifiability structure of spiral-time models by establishing operational criteria and no-go conditions for memoryless temporal dynamics under controlled intervention protocols [26]. These developments provide a clearer experimental pathway for distinguishing intrinsic temporal-memory effects from conventional Markovian dynamics.

From a computational perspective, the proposed framework is lightweight. The spiral-time operator acts directly on existing time-series data and does not require large-scale neural network training. Standard spectral and phase-coherence methods are sufficient for implementation, which makes the approach potentially suitable for real-time or clinical applications, pending further validation.

4. Code and Independent Validation

Independent validation and reproducibility material related to this manuscript is available as an executable Jupyter notebook containing EEG-based analyses corresponding to the neurodynamic collapse framework discussed in this work. The underlying theoretical framework (Unified Spiral-Time Dynamics) was publicly disclosed prior to the EEG validation study and assigned a persistent DOI. The subsequent experimental validation therefore represents an application and empirical test of this framework rather than an independent theoretical origin.

For transparency and reproducibility, the analytical implementation and validation materials are available in a public software repository:
https://github.com/nwycomp/NeuroDynamics-Collapse-Validation-/blob/main/eeg-part-four.ipynb

A citable archival version of the associated validation dataset is available via Zenodo:

Krüger, M. (2025). *Validation dataset*. Zenodo. https://doi.org/10.5281/zenodo.17990696

5. Conclusion

This work presented a unified information-theoretic framework for neural coherence based on triadic spiral-time dynamics within the HLV theory. By integrating the spiral-time operator structure with the DLHR multi-layer psychological architecture and neurophotonically motivated coupling terms, a single dynamical formalism was derived that links emotional regulation, identity formation, memory dynamics, and coherent neural activity.

The central contribution of this study is the formulation of a mathematically consistent evolution equation that unifies cognitive, emotional, and biophysical processes within a common geometric framework. The model yields concrete, falsifiable predictions for neural phase coherence, trauma-related attractor dynamics, and biophotonic coupling effects, providing clear pathways for experimental and clinical investigation. These predictions provide clear opportunities for independent experimental verification using EEG, MEG, and related phase-coherence measurement techniques.

While the present work is primarily theoretical, it establishes a structured foundation for future empirical validation using EEG, MEG, NV-center sensing, and related measurement techniques. More broadly, the framework demonstrates how information geometry, coherence, and multi-layer temporal structure can jointly account for complex neurodynamic phenomena. Taken together, these results suggest that spiral-time dynamics may provide a promising route toward a physically grounded theory of neural coherence and cognitive organization.

Ethical Statement

This study does not involve human participants, animals, or the use of any personal or identifiable data. No ethical approval or informed consent was required for this work.

Conflicts of Interest

The authors declare that they have no known competing financial interests or personal relationships that could have appeared to influence the work reported in this paper.

Data Availability Statement

The analytical implementation and validation materials related to this manuscript are available in a public software repository: https://github.com/nwycomp/NeuroDynamics-Collapse-Validation-/blob/main/eeg-part-four.ipynb. A citable archival version of the associated validation dataset is available via Zenodo: https://doi.org/10.5281/zenodo.17990696.

Author Contribution Statement

Marcel Krüger: Conceptualization, Methodology, Formal analysis, Writing – original draft, Visualization, Supervision, Project administration. **Don Feeney:** Conceptualization, Writing – review & editing. **Marcel Theodor Wende:** Conceptualization, Investigation, Writing – review & editing.

References

[1] Stein, A. G., & Pollak, S. D. (2024). Computational modeling approaches to emotional development. *Developmental Psychology*, *61*(4), 679–690. https://doi.org/10.1037/dev0001830

[2] Borsboom, D., van der Maas, H. L. J., Dalege, J., Kievit, R. A., & Haig, B. D. (2021). Theory construction methodology: A practical framework for building theories in psychology. *Perspectives on Psychological Science*, *16*(4), 756–766. https://doi.org/10.1177/1745691620969647

[3] Benton, D. T. (2023). But What Is the Mechanism? Demystifying the ever elusive 'developmental mechanism. *Infant and Child Development*, *32*(6), e2355. https://doi.org/10.1002/icd.2355

[4] Luppi, A. I., Cabral, J., Cofré, R., Destexhe, A., Deco, G., & Kringelbach, M. L. (2022). Dynamical models to evaluate structure–function relationships in network neuroscience. *Nature Reviews Neuroscience*, *23*, 767–768. https://doi.org/10.1038/s41583-022-00646-w

[5] van Rooij, I., & Baggio, G. (2021). Theory before the test: How to build high-verisimilitude explanatory theories in psychological science. *Perspectives on Psychological Science*, *16*(4), 682–697. https://doi.org/10.1177/1745691620970604

[6] Houlihan, S. D., Kleiman-Weiner, M., Hewitt, L. B., Tenenbaum, J. B., & Saxe, R. (2023). Emotion prediction as computation over a generative theory of mind. *Philosophical Transactions of the Royal Society A*, *381*(2251), 20220047. https://doi.org/10.1098/rsta.2022.0047

[7] Ruba, A. L., Pollak, S. D., & Saffran, J. R. (2022). Acquiring complex communicative systems: Statistical learning of language and emotion. *Topics in Cognitive Science*, *14*(3), 432–450. https://doi.org/10.1111/tops.12612

[8] Teo, D. W. H., Ang, Z. Y., & Ong, D. (2022). Modeling causal inference from emotional displays. In Toronto, Canada, *Proceedings of the Annual Meeting of the Cognitive Science Society*. 2022 https://escholarship.org/uc/item/3w06g892

[9] Krüger, M. (2025). Quantization of spiral-time dynamics in the HLV theory. *Zenodo*. https://doi.org/10.5281/zenodo.17296261

[10] Brigham, E. O. (1988). *The fast fourier transform and its applications*. USA: Prentice-Hall.

[11] Liska, M., Hesp, C., Tchekhovskoy, A., Ingram, A., van der Klis, M., & Markoff, S. (2018). Formation of precessing jets by tilted black hole discs in 3D general relativistic MHD simulations. *Monthly Notices of the Royal Astronomical Society: Letters*, *474*(1), L81–L85. https://doi.org/10.1093/mnrasl/slx174

[12] Rakovszky, T., Gopalakrishnan, S., & von Keyserlingk, C. (2024). Defining stable phases of open quantum systems. *Physical Review X*, *14*, 041031. https://doi.org/10.1103/PhysRevX.14.041031

[13] Stojnic′, G., Gandhi, K., Yasuda, S., Lake, B. M., & Dillon, M. R. (2023). Commonsense psychology in human infants and machines. *Cognition*, *235*, 105406. https://doi.org/10.1016/j.cognition.2023.105406

[14] Geraci, A., Simion, F., & Surian, L. (2022). Infants' intention-based evaluations of distributive actions. *Journal of Experimental Child Psychology*, *220*, 105429. https://doi.org/10.1016/j.jecp.2022.105429

[15] Perets, H. B., Li, Z., Lombardi, J. C., & Milcarek, S. R. (2016). Micro-tidal disruption events and the production of ultra-long GRBs. *The Astrophysical Journal*, *823*(2), 113. https://doi.org/10.3847/0004-637X/823/2/113

[16] Huebner, M., Huppenkothen, D., Lasky, P. D., & Inglis, A. R. (2022). Pitfalls of periodograms: The nonstationarity bias in the analysis of quasiperiodic oscillations. *The Astrophysical Journal Supplement Series*, *259*(2), 32. https://doi.org/10.3847/1538-4365/ac49ec

[17] Huppenkothen, D., Baring, M. G., Uzuner, M., Gögüs, E., Kaneko, Y., Kouveliotou, C., . . . , & Lin, L. (2025). Searching for quasi-periodicities in short transients: The curious case of GRB 230307A. *Astronomy and Astrophysics*, *702*, A149. https://doi.org/10.1051/0004-6361/202553952

[18] Walle, E. A., Lopez, L. D., & Castillo, A. (2022). Emotional development: A field in need of a (cognitive) revolution. In D. Dukes, A. C. Samson, & E. A. Walle (Eds.), *The Oxford Handbook of Emotional Development* (*(pp. 61–77)*). Oxford University Press. https://doi.org/10.1093/oxfordhb/9780198855903.013.16

[19] Wu, Y., Schulz, L. E., Frank, M. C., & Gweon, H. (2021). Emotion as information in early social learning. *Current Directions in Psychological Science*, *30*(6), 468–475. https://doi.org/10.1177/09637214211040779

[20] Woo, B. M., Liu, S., & Spelke, E. S. (2024). Infants rationally infer the goals of other people's reaches in the absence of first-person experience with reaching actions. *Developmental Science*, *27*(3), e13453. https://doi.org/10.1111/desc.13453

[21] Bhat, P. N., Meegan, C. A., von Kienlin, A., Paciesas, W. S., Briggs, M. S., Burgess, J. M., . . . , & Zhang, B. (2016). The third fermi GBM gamma-ray burst catalog: The first six years. *Astrophysical Journal Supplement Series*, *223*(2), 28. https://doi.org/10.3847/0067-0049/223/2/28

[22] Goldberger, A. L., Amaral, L. A., Hausdorff, J. M., Ivanov, P. Ch., Peng, C. K., & Stanley, H. E. (2002). Fractal dynamics in physiology: Alterations with disease and aging. *Proceedings of the National Academy of Sciences of the United States of America*, *99*(Suppl 1), 2466–2472. https://doi.org/ 10.1073/pnas.012579499

[23] Malik, M. (1996). Heart rate variability: Standards of measurement, physiological interpretation, and clinical use. *Circulation*, *93*, 1043–1065.

[24] Arch, M., Rosenblum, M. G., Pikovsky, A. S., & Kurths, J. (1996). Phase synchronization of chaotic oscillators. *Physical Review Letters*, *76*, 1804–1807. https://doi.org/10.1103/PhysRevLett.76.1804

[25] Krüger, M., & Feeney, D. (2026). A spiral-time operator framework for heart–brain isostasis: Operator-based early detection of cardiac instability. *Zenodo*. https://doi.org/10.5281/zenodo.18213656

[26] Krüger, M. (2026). Spiral-Time with memory as a fundamental principle: From non-markovian dynamics to measurement without collapse. *Zenodo*. https://doi.org/10.5281/zenodo.18698175

How to Cite: Krüger, M., Feeney, D., & Wende, M. T. (2026). Information-Theoretic Modeling of Neural Coherence via Triadic Spiral-Time Dynamics: A Framework for Neurodynamic Collapse. *Medinformatics*. https://doi.org/10.47852/bonview62029043